

## On the Globular Cluster IMF below $1 M_{\odot}$ <sup>1</sup>

Francesco Paresce and Guido De Marchi

European Southern Observatory, Karl-Schwarzschild Strasse 2, D-85748 Garching,  
Germany

fpiresce@eso.org, demarchi@eso.org

### ABSTRACT

Accurate luminosity functions (LF) for a dozen globular clusters have now been measured at or just beyond their half-light radius using HST. They span almost the entire cluster main sequence (MS) below  $0.75 M_{\odot}$ . All these clusters exhibit LF that rise continuously from an absolute  $I$  magnitude  $M_I \simeq 6$  to a peak at  $M_I \simeq 8.5-9$  and then drop with increasing  $M_I$ . Transformation of the LF into mass functions (MF) by means of the mass luminosity (ML) relations of Baraffe et al. (1997) and Cassisi et al. (1999) that are consistent with all presently available data on the physical properties of low mass, low metallicity stars shows that all the LF observed so far can be obtained from MF having the shape of a log-normal distribution with characteristic mass  $m_c = 0.33 \pm 0.03 M_{\odot}$  and standard deviation  $\sigma = 1.81 \pm 0.19$ . In particular, the LF of the four clusters in the sample that extend well beyond the peak luminosity down to close to the Hydrogen burning limit (NGC 6341, NGC 6397, NGC 6752, and NGC 6809) can only be reproduced by such distributions and not by a single power-law in the  $0.1 - 0.6 M_{\odot}$  range. After correction for the effects of mass segregation, the variation of the ratio of the number of higher to lower mass stars with cluster mass or any simple orbital parameter or the expected time to disruption recently computed for these clusters by Gnedin & Ostriker (1997) and Dinescu et al. (1999) shows no statistically significant trend over a range of this last parameter of more than a factor of  $\sim 100$ . We conclude that the global MF of these clusters have not been measurably modified by evaporation and tidal interactions with the Galaxy and, thus, should reflect the initial distribution of stellar masses. Since

---

<sup>1</sup>Based on observations with the NASA/ESA *Hubble Space Telescope*, obtained at the Space Telescope Science Institute, which is operated by AURA, Inc., under NASA contract NAS5-26555

the log-normal function that we find is also very similar to the one obtained independently for much younger clusters and to the form expected theoretically, the implication seems to be unavoidable that it represents the true stellar IMF for this type of stars in this mass range.

*Subject headings:* stars: stars: luminosity function, mass function – Galaxy: globular clusters, open clusters

## 1. Introduction

The IMF is a critical ingredient in our understanding of a large number of basic astronomical phenomena such as the formation of the first stars, galaxy formation and evolution, and the determination of the absolute star formation rate. It also plays a dominant role in any star formation theory as the end result of molecular cloud contraction and fragmentation. Moreover, the IMF is one of the important factors determining the rate of cluster disruption via internal and external evolution (relaxation and tidal shocking) and, in consequence, of the possible dark matter content of galaxy halos. In this latter context, a single power law IMF increasing as  $dN/dm \propto m^{-\alpha}$  with  $\alpha \gtrsim 2$  all the way to very low substellar masses is required to substantially affect the baryonic mass budget of the halo (Chabrier & Méra 1997; Graff & Freese 1996).

The actual measurement of a MF is a complex process whose ultimate precision and reliability rests heavily on a very careful quantitative analysis of all sources of possible random and systematic error. The basic uncertainties presently stem mainly from sample contamination, incompleteness, errors in the mass-luminosity and color-magnitude relations, the age, distance, and extinction of the stars, their evolution, mass segregation, and unresolved binaries. The IMF itself depends crucially, in most cases, on knowledge of the age and on any subsequent effects such as external dynamical evolution of a cluster in a galactic tidal field. For all these reasons, it has proven very difficult to pin down the shape of the IMF observationally with the required reliability and accuracy in a wide variety of stellar environments (Scalo 1998, 1999). The slope of the MF at the lowest mass end of the stellar MS and, in particular, whether or not there is a turn-over at the lowest masses before the H-burning limit and whether or not the IMF is universal or rather depends on the initial physical conditions in the natal environment are critical open issues at present.

Globular clusters represent, in principle, the ideal sample from which to deduce the stellar IMF and properly answer the above questions. They offer a large statistically significant sample of relatively bright, coeval, equidistant stars with, in most cases, relatively small

variations of chemical composition and extinction within each cluster. They were all formed very early in the history of the Galaxy and there is no evidence of subsequent star formation episodes. The binary fraction outside the core is less than 10 – 15 % and has an insignificant effect on the measured LF (Rubenstein & Bailyn 1999). Mass segregation is a relatively straightforward and well understood phenomenon quantifiable by simple Michie–King models such as those used by Meylan (1987, 1988). The only potentially serious obstacle is related to the possible modification of the IMF by the effect of tidal interactions with the Galaxy potential. This interaction, integrated over the orbit and time, is expected to slowly decrease the slope of the global mass function of the cluster (Vesperini 1998) thereby effectively masking the original IMF from our present day observations, no matter how precise and detailed they are.

Since deep LF of a dozen globular clusters (GC) in our Galaxy have now been accurately measured, we are in a good position to address observationally the issue of if and, possibly, how the interaction history of these clusters, whose Galactic orbits are reasonably well known, affects their LF in the mass range where the signature is expected to be most significant. In this paper, we show that LF obtained at or just beyond the half-light radius of these clusters surveyed are completely insensitive to this history and that they can indeed be used to deduce an uncontaminated stellar IMF below  $1 M_{\odot}$  for these stars.

## 2. Observational Data

The main characteristics of the data used for this study are summarized in Table 1 and their relevant presently available physical parameters are listed in Table 2. All the listed clusters have well measured LF in the critical range  $6.5 < M_I < 10$  and some even well beyond these limits. We have restricted this study to absolute  $I$  magnitudes greater than 4.5 corresponding to a mass of  $\sim 0.75 M_{\odot}$  to avoid the mass range near the turn-off where cluster age and instrument saturation might significantly affect the determination of the LF (Silvestri et al. 1998; Baraffe et al. 1997; De Marchi et al. 1999). The LF of these clusters in number per 0.5 magnitude bins as determined by analysis of their color–magnitude diagrams (CMD) are plotted with the relevant  $1 \sigma$  error-bar in Figure 1, as a function of the absolute  $I$ -band magnitude obtained using the distance moduli given in Table 2.

The statistical errors shown in Figure 1 have been determined by combining in quadrature the uncertainty resulting from the Poisson statistics of the counting process with that accompanying the measurement of the photometric incompleteness. The family of curves shown in Figure 1 represents a very homogeneous sample of objects all observed and analyzed with the same basic techniques well outside the core in a region where the low-mass

MS is well populated. The most obvious feature of the observed LF is the peak located at  $M_I \simeq 8.5 - 9$  with a rising and descending part on each side. Only the clusters NGC 6341, NGC 6397, NGC 6656, NGC 6752, and NGC 6809 extend significantly beyond  $M_I = 10$  in this sample due to the difficulty of obtaining reliable LF at such faint luminosities for the more distant objects.

### 3. Conversion to a Mass Function

The observed local LF (i.e.  $dN/dM_I$ ) shown in Figure 1 can be converted into the corresponding MF (i.e.  $dN/d \log m$ ) by the application of a mass-luminosity relation (ML) as follows:

$$dN/dM_I = dN/d \log m \times d \log m/dM_I \quad (1)$$

Thus, the observed LF is simply the product of the MF with the derivative of the ML relation. The critical step here, therefore, is intimately connected to the proper realization of the appropriate ML relation for the age and metallicity of the cluster. A number of possibilities exists presently but the most reliable are the theoretical ML relations explicitly computed for the appropriate observational bandpasses by Alexander et al. (1997), Silvestri et al. (1998), Baraffe et al. (1997, 1998) and Cassisi (1999). Subtle differences between the calculations can be considerably amplified by the derivative process that is required to transform a LF into a MF and vice versa as shown in Equation 1. The main reason for these differences lies in the use of the gray atmosphere approximation in the first two models while the Baraffe et al. (1997) and Cassisi (1999) approach relies on a self-consistent non-gray model atmosphere to provide the correct boundary conditions for the interior integration (Chabrier, Baraffe, & Plez 1996). Another reason is probably connected to the differing equations of state used by the different authors. In any case, the very fact that there are significant differences in the various approaches that could definitely affect the final transformation strongly argues that we should use the models that adopt the fewest approximations to the physical processes underlying the emitted spectrum and that adequately fit the widest possible range of available data on low mass, low metallicity stars with the minimum of adjustable parameters. Presently, this advantage lies with the Baraffe et al. (1997; see Chabrier et al. 1999 for the most recent review) and Cassisi (1999) models that we, therefore, will use exclusively in the following discussion. The two models are, fortunately, practically indistinguishable from one another in the I band and our mass range. This consistency between independent determinations increases our confidence in the basic reliability of the M-L relation used here.

Since it is common practice to derive a MF from a given LF by dividing the latter by the derivative of the ML relation, in principle we could apply Equation 1 to the data in Figure 1 and derive the MF directly through the inversion of the LF. In this way, however, the contribution of the experimental errors and of the uncertainties inherent in the models would become difficult to disentangle in the final result. Instead, we prefer to assess the validity of a model MF by converting it into the observational plane and comparing directly the resulting LF with the observed one, precisely as indicated by the formalism of Equation 1. Particular care should be used, however, when assuming a functional form for the MF. Since the MF is often defined as the differential probability distribution of stellar mass  $m$  per unit logarithmic mass range, i.e.  $F(\log m)$ , it is convenient to use the logarithmic index  $-x = d \log F(\log m) / d \log m$  to characterize the MF slope locally, over a narrow mass interval. As Scalo (1998) points out, however, this characterization might seem to imply that the MF is a power law with fixed index  $x$ , and thus it might seem to justify extending over a wide mass range an index derived over a much narrower mass interval. This assumption is probably responsible for much of the confusion still affecting the shape of the MF of GC stars near the H-burning limit.

In fact, as recently shown by De Marchi, Paresce, & Pulone (2000), the deepest LF available for NGC 6397 rules out the possibility that its MF is represented by a power-law distribution with a single value of the exponent  $x$ . We refer the reader to that paper for a complete discussion of the details, but report here the main points of that derivation for sake of clarity:

1. The expected V and I magnitudes and colors from Baraffe et al. (1997, 1998) appropriate to the distance, age, and metallicity of NGC 6397 fit very well the observed optical and near-IR CMD with no adjustable parameters;
2. The LF of this cluster has now been observed by three different techniques from the optical to the near IR by two different groups all of which give the same result throughout the wide luminosity range between  $6.0 \lesssim M_I \lesssim 12.5$  within observational errors;
3. The resulting MF cannot be reproduced by a single power-law function over this range as shown in Figure 2, because after multiplication with the appropriate ML relation such a function cannot simultaneously fit both the rising and descending portions of the LF;
4. The mass function that best fits the combined data on NGC 6397 is a log-normal distribution (see Equation 2) with mass scale  $m_c \simeq 0.3$  and standard deviation  $\sigma \simeq 1.7$ . The LF to which this MF gives rise is shown as a dashed curve in the bottom panel of Figure 2.

We cannot claim, of course, that all the other clusters in our study, and especially those whose observed LF do not extend as far beyond  $M_I \simeq 10$  in Figure 1 as NGC 6397, have to have their MF in the shape of that of NGC 6397 necessarily, since we do not yet have data in the fainter regime. They might have continuously rising MF down to the H-burning limit as espoused by Chabrier & Méra (1997), for example, but the ascending parts are essentially indistinguishable from one another and the implication at least is that they would have a similar behavior below the peak. This is certainly true for NGC 6656 as discussed in De Marchi & Paresce (1997) as well as for NGC 6341, NGC 6752, and NGC 6809 since their LF extend to  $M_I = 11$  well beyond the peak and are not compatible with an underlying power-law MF, regardless of the value of its index  $x$ .

In Figure 3, we show the log-normal distributions that accurately reproduce the LF plotted in Figure 1 over the whole magnitude range spanned by the observations. Solid lines mark the portion of the MF that have been fitted to the data, while the dashed lines represent the extrapolation of the same MF to fill in the range  $0.09 - 0.7 M_\odot$ . The dashed lines in Figure 1 represent the theoretical LF obtained with the MF shown in Figure 3 that best fit the observed LF. The log-normal MF is characterized by only two parameters namely the characteristic mass  $m_c$  and the standard deviation  $\sigma$  and takes on the form:

$$\ln f(\log m) = A - \frac{[\log(m/m_c)]^2}{2\sigma^2} \quad (2)$$

where  $A$  is a normalization constant. The average values of the parameters for this sample of clusters are  $\langle m_c \rangle = 0.33 \pm 0.03$  and  $\langle \sigma \rangle = 1.81 \pm 0.19$ . The uncertainties accompanying  $\langle m_c \rangle$  and  $\langle \sigma \rangle$  represent the scatter of the individual values of  $m_c$  and  $\sigma$  which are given for each cluster in Table 2. It should be noted that the relatively small values of  $\sigma$  in Table 2 imply that for  $m < m_c$  the MF drops not only in the logarithmic plane, but also in linear units, i.e. the number of stars per unit mass *decreases with decreasing mass below the peak*. A simple, unbiased measure of the steepness of the rise to the maximum of the MF shown in Figure 3 that does not depend on any preconceived notion on the shape of the MF is  $\Delta \log N$ , defined as the logarithmic ratio of the number of lower to higher mass stars taken from the MF in the mass range between  $m = m_c$  and  $m = 0.7 M_\odot$ . This is probably the most convenient parameter to describe the region of the mass distribution most likely to be affected by external and internal dynamics and is listed in Table 2 for each cluster. Another advantage of  $\Delta \log N$  is that it is defined in a mass range where the stellar surface structure is best understood and all presently available models for the ML relation are in good agreement with each other (Silvestri et al. 1998) and is, in consequence, least likely to be subject to uncertainties due to the LF to MF conversion.

#### 4. Correction for Mass Segregation

The MF shown in Figure 3 need to be corrected for the effects of mass segregation due to energy equipartition as has been extensively discussed in Pulone et al. (1999), for example, in the case of NGC 6121 (M4). To assess the magnitude of the expected effect on the shape of the local MF, we have run standard multi-mass Michie–King models for the clusters in our sample. As a typical example, in Figure 4 (left panel), the expected local MF is plotted as a function of radial position and compared to the input global MF (dashed lines) for the case of NGC 6397. As can be seen in this figure, the largest departure of the local MF from the global MF occurs in the innermost regions of the cluster ( $r \lesssim 0.1r_h$ ) but significant deviations also occur beyond the half-light radius. Near the half-light radius the deviations are insignificant. This is shown graphically in the right panel of Figure 4, where we plot the standard deviation of the local from the global MF as a function of radial position for this cluster. These results are quite consistent with the expectations of previous work along these lines by Richer et al. (1991) and Pryor, Smith, & McClure (1986).

It is clear from this result that, provided the measurements are carried out close to the half-light radius where the effects of mass segregation are minimal, the deviation between the local MF and the global one is basically unmeasurable with present techniques. This result was confirmed for NGC 6397 where the global MF was found to be essentially indistinguishable from the MF determined at the half light radius (De Marchi et al. 2000). While the majority of the LF in our sample fulfill this requirement and can, therefore, be left safely unaltered, those of NGC 6341, NGC 7078, and NGC 7099 have been obtained farther out in the cluster, at about  $\sim 4r_h$  (see Table 1) in a region where the deviations can be significant as indicated in Figure 4. The effects of mass segregation must be accounted for in these cases as they might otherwise lead to global MF that appear steeper than they really are. The corrected  $\Delta \log N$  for these clusters obtained by using the appropriate Michie–King models are listed in Table 2. The effect of this correction is a decrease, as expected, of the value of  $\Delta \log N$  for all three clusters.

#### 5. Physical Data and Tidal Disruption

In Table 2, we list the main physical parameters of the clusters surveyed so far. Since our main objective is to search for a signature of the cluster’s dynamical history on its low mass MF, we have included in this table whatever is known about its orbit in the Galactic tidal field. The space motion data were obtained from the work of Dauphole et al. (1996), Odenkirchen et al. (1997), and Dinescu, Girard, & Van Altena (1999). These data can be used in a theoretical model to determine the change with time of the cluster’s main

characteristics such as total mass, mass and luminosity functions, tidal radii, central concentrations, relaxation times, etc. Both N-body and Fokker-Planck models of increasing sophistication have been used recently to compute such evolution (Takahashi & Portegies Zwart 1999; Gnedin, Hernquist, & Ostriker 1999; Vesperini 1998, 1997; Vesperini & Heggie 1997; Gnedin & Ostriker 1997; Capriotti & Hawley 1996; Murali & Weinberg 1997). Although different authors use different initial conditions and approximations to the complex tidal interaction mechanisms, the generally physically plausible final result is a flattening of an assumed power-law low mass MF with time due to the preferential evaporation of lower mass stars forced by two-body relaxation out to the cluster periphery where the evaporation process is accelerated by tidal shocks.

A direct calculation of this phenomenon for a specific cluster orbit has not been carried out yet but an indirect indication at least of the magnitude of the effect can be gleaned from the recent calculations of the time to disruption  $T_d$  of specific clusters carried out by Gnedin & Ostriker (1997) and by Dinescu et al. (1999). These times are given in Gyr in Table 2 (assuming a value of 10 Gyr for a Hubble time) where the two values of the total destruction rate given by Gnedin & Ostriker (1997) for the two galactic models used in their calculations have been averaged in column (10). The observed clusters cover quite a large range of  $T_d$  from a minimum of 4 Gyr for NGC 6397 to 213 Gyr for NGC 5272 (using Gnedin & Ostriker’s values), or from 2 Gyr for NGC 6121 to 275 Gyr for NGC 5272 (following Dinescu et al. 1999). These values should in principle be regarded as upper limits to the true  $T_d$ , as both Gnedin & Ostriker and Dinescu et al. treat the internal dynamical evolution of the clusters by using single-mass Michie–King models and, thus, tend to underestimate the effects of mass segregation. Although differences exist between the values of  $T_d$  as given by Gnedin & Ostriker and Dinescu et al. (with the latter being usually larger), an inspection of Table 2 shows that no one particular orbital parameter or the cluster mass by itself is sufficient to foretell what the fate of the cluster will be. Even, for example, the cluster’s perigalactic distance or its height above the plane are not well correlated with  $T_d$ . This means that the overall impact of the repeated bulge and disk shocks on the cluster over its lifetime is not easily predictable from a simple glance at the orbital parameters but only from the use of calculations over the entire orbit such as those referred to above.

All things being equal, then, we would expect that the clusters with the largest times to destruction  $T_d$ , i.e. those that have suffered the least tidal disruption, to have the largest low to high mass number ratio  $\Delta \log N$ . The actual situation is shown in Figure 5 where we have plotted the time to disruption of Gnedin & Ostriker (1997) as a function of  $\Delta \log N$ . The best linear fit to this distribution is a straight line with zero abscissa at  $T_d = 113 \pm 3$  and having a slope of  $-2.9$  with a formal error of  $\pm 0.2$ . A horizontal line drawn at  $\log T_d \simeq 1.5$ , however, would still give an acceptable fit. Within the errors, then, there is no discernible

trend in this direction and the conclusion at this point is, therefore, quite clear: the global MF of the clusters in our sample show no evidence of evolution with time within the quoted errors.

The MF logarithmic ratios  $\Delta \log N$  plotted in Figure 5 do seem to have a statistically significant scatter about the mean beyond that expected from measurement errors alone. What this scatter is due to is not at all clear at the moment since we cannot simply ascribe it to tidal effects. Intrinsic variations of the observed magnitude in the IMF slope in this mass range are generated naturally in Adams & Fatuzzo’s (1996) hypothesis due to variations in conditions under which accretion is choked off by the appearance of winds from the proto-star. The same effect is predicted by Elmegreen’s (1999a, 1999b) hierarchical cloud sampling model due to both the inherently random sampling process and the variation of the thermal Jeans mass with initial conditions. If confirmed with more precise data, this effect, if real, may be a sensitive indicator of natal cloud conditions such as temperature and pressure.

In light of the very small range spanned by  $m_c$  and  $\sigma$  deduced for all our clusters, the conclusion is, then, that a single form of the MF can easily reproduce all the 12 deep LF obtained so far and, since there is no obvious dependence on dynamical history over an extremely wide range of conditions, that this MF is most likely to represent the initial distribution of stellar masses in the cluster, namely the IMF.

Finally, we should note that, although we have argued on the basis of the data presented above that there seems not to be any, as yet, measurable effect of tidal interactions with the galaxy showing up at or just beyond the half-light radius and implying a massive ongoing disruption event in any of the 12 clusters in our sample, there is evidence of this effect in the LF of NGC 6712 as recently measured with the VLT (De Marchi et al. 1999). This cluster’s MF, if extrapolated to the relevant mass range of the others, would show a  $\Delta \log N \simeq -0.1$ . This result implies that some clusters are much more capable than others in shielding their interiors very effectively from tidal disruption while others, like NGC 6712 are very vulnerable to this effect.

How this may work in practice is starting to be understood by recent theoretical and numerical simulation studies (Takahashi & Portegies Zwart 1999; Gnedin, Hernquist & Ostriker 1999). For example, such calculations do predict that most of the clusters in our present sample are quite stable being located well inside the survival boundaries of the vital diagrams plotted by Gnedin & Ostriker (1997). They may have survived so far relatively undisturbed in the interior at least due to special initial conditions (high mass and concentration) and a relatively benign shock history even though their outer parts may well show indications of tidal heating (Drukier et al. 1998; Leon, Meylan & Combes 1999). In any case, they are unlikely to have lost more than  $\sim 1\%$  of their mass due to tidal shocking (Combes,

Leon & Meylan 1999). NGC 6712, on the other hand, may be one of the few caught in the brief period before complete disruption. Takahashi & Portegies Zwart (1999) predict that, initially, NGC 6712 had more than 1000 times its present mass.

## 6. Discussion

### 6.1. Comparison with Previous Work

A preliminary comparison of the properties of the first deep cluster LF measured with the HST was carried out by De Marchi & Paresce (1997, and references therein). In those papers, we showed that the shape of the LF, all measured near the half-light radius, seemed to bear little or no relation with the past dynamical history of the clusters nor with their position in the Galaxy. In spite of the widely different dynamical properties of the low-metallicity clusters NGC 6397, NGC 6656, and NGC 7078, near their half-light radius these three objects feature what in practice is the same LF below  $\sim 0.6 M_{\odot}$  (see Figure 1). Our conclusions, then, on the basis of a much more limited data base and uncertain models were fortuitously substantially similar to those in this paper.

From their comparison of the LF of nine clusters (all of which are also part of the present study), Chabrier & Méra (1997) concluded that the MF of GC is “well described by a slowly rising power-law  $dN/dm \propto m^{-\alpha}$  with  $0.5 \lesssim \alpha \lesssim 1.5$  down to  $0.1 M_{\odot}$ ,” at variance with what we show in Figure 3. Several factors might be at the origin of this discrepancy. First, in order to compare LF measured in different wavelength bands, Chabrier & Méra converted them all into bolometric luminosities. Although the claim is that the LF of the same cluster observed through different filters should yield the same bolometric LF, mixing data with theory makes the true uncertainty much more difficult to estimate. Second, two of the LF that they used are now known to be incorrect at the low mass end, namely that of NGC 6397 of Cool et al. (1996) later amended in King et al. (1998) and that of NGC 5139 measured by Elson et al. (1995) and recently corrected by De Marchi (1999). Both LF overestimated the number of objects below  $\sim 0.3 M_{\odot}$ , thus mimicking an increase in the MF where a flattening should have occurred instead.

A third effect, partly ensuing from the second, is that, having noticed the discrepancy existing then between the LF of NGC 6397 of Cool et al. and that of Paresce et al. (1995) at the low mass end, Chabrier & Méra were forced to exclude NGC 6397 from their analysis. But since the LF of NGC 6397 reaches the faintest luminosities observed so far, ignoring it prevents a reliable determination of the MF at the lowest mass end. Finally, they also ignore the flattening of the MF of NGC 6656 and NGC 6341 below  $0.2 M_{\odot}$ . All of this, combined

with the considerable structure that one sees in the MF above  $\sim 0.3 M_{\odot}$ , makes any claim based on a single exponent power-law mass distribution extending all the way to  $\sim 0.1 M_{\odot}$  for GC presently unsustainable. The only way to modify this conclusion would be to assume an error in the Baraffe et al. (1997) and Cassisi (1999) ML relations at the lowest masses. The only known reason for a discrepancy would be in the possible formation of dust in the atmosphere but this effect should be minimal in stars of such a low metallicity.

Piotto et al. (1997) have also noticed the unsuitability of a single power-law distribution to represent the MF of GC. In fact, the MF that they obtain by applying the ML relation of D’Antona & Mazzitelli (1995) or that of Alexander et al. (1997) to their LF deviate from a single exponent power-law, even when they restrict their investigation to the small mass range below  $\sim 0.4 M_{\odot}$ . As Figure 5 and Table 2 clearly show, this is not unexpected because the peak of the MF is located at  $m_c \simeq 0.33 M_{\odot}$ . A drop-off below the peak at  $\sim 0.3 M_{\odot}$  is also found by King et al. (1998) whose LF, if anything, is slightly steeper than ours (see the comparison shown in Figure 5 of De Marchi et al. 2000).

Piotto & Zoccali (1999) again use a power-law fit to the MF of a larger sample of clusters — even if strong departures from a pure power-law distribution are clearly evident at both the higher and lower mass ends — to claim the existence of a correlation between the rate of destruction of their sample of clusters with the slope of their best fit power law to the MF. On the other hand, restricting, for example, Figure 5 only to the clusters studied by Piotto & Zoccali (1999) would not show any correlation between the time to disruption of a cluster with  $\Delta \log N$ . The reason for this discrepancy is not clear but it may have to do with a combination of smaller sample, a power law slope that bears little relation with the mass distribution of the stars in the clusters, and rough estimates of the effects of mass segregation. This last point is absolutely essential for proper inter-cluster comparisons especially in view of the fact that most HST–WFPC 2 LF tend to be taken at constant sky offsets ( $\sim 4'.5$ ) from the core and that, therefore, the farther away the cluster the farther out physically is the LF sampled and the segregation correction greatest.

Another problem commonly encountered in this type of work is that what seem like significant differences in the LF are almost completely washed out in the MF from which they descend especially once the effects of mass segregation are accounted for. Thus, no meaningful comparison between clusters can be made on the basis of the LF alone and, since possible effects of evaporation are impressed on the MF, it is exclusively in this plane that they must be sought.

Finally, Silvestri et al. (1998) argue that the MF of the entire MS of NGC 6397 is consistent with a shallow slope power-law if their most recent models for the ML relation are used to convert the cluster LF shown in Figure 1. As these authors point out, this is due

to their ML relation being steeper than that of Baraffe et al. (1997) at the low end of the MS. As we already mentioned above, these models rely on a grey atmosphere approximation that is not self-consistent and that, therefore, cannot be preferred to the latter that rely on a completely self-consistent approach which provides excellent matches to a wide variety of experimental data.

Silvestri et al. (1999) also address the issue of how a change in the distance scale of globular clusters will affect their MF, showing that longer distances result in shallower MF, or, better, in a more pronounced flattening at the low-mass end. In view of the still debated revision of the distances to globular clusters based on the new Hipparcos data (see e.g. Gratton et al. 1997; Pont et al. 1997), we have adopted the pre-Hipparcos values in our analysis. Nevertheless, since the distance moduli of the 9 globular clusters studied by Gratton et al. (1997) are in excess of those of Djorgovski (1993) by only  $0.22 \pm 0.10$  mag, using the new scale would not change our results significantly.

## 6.2. Comparison with Other Clusters

How does the globular cluster IMF derived here compare with MF derived in other stellar clusters? The present situation in this regard is summarized in Figure 6 where we have drawn the most recently deduced MF in several Galactic cluster populations. The data are for the Orion Nebula Cluster from Hillenbrand (1997), IC348 from Luhman et al. (1998) and Herbig (1998), the Pleiades as reported by Bouvier et al. (1998), and the Hyades from Reid & Hawley (1999) and Gizis, Reid & Monet (1999). For comparison, the MF deduced from the NGC 6397 LF shown in Figure 3 is also reproduced here in the same format. Since the Galactic halo may well be populated mainly by the disruption of globular clusters, we also show in this figure the MF of the halo as obtained from the LF of Dahn et al. (1995) confirmed by Fuchs & Jahreiss (1998) and Gizis & Reid (1999), converted to a MF by Chabrier & Méra (1997), and corrected for binaries by Graff & Freese (1996).

The measurement peculiarities and sources of uncertainties in these measurements are exhaustively discussed and quantitatively evaluated by these authors so that they should be regarded as the most precise and up to date determinations of the MF in the  $\sim 0.1 - 3 M_{\odot}$  mass range. We have distilled their measurements into the best fitting power law in the appropriate mass range. The data are shown in logarithmic mass units on the abscissa and the MF represented as the  $\log dN/d \log m$  in the ordinate. The slope of the power law is then  $-x = 1 - \alpha$  where  $\alpha$  is the slope in linear mass units ( $\alpha = 2.35$  for the Salpeter IMF). The vertical position of the lines is arbitrary, of course, so we have shifted them up or down for enhanced visibility.

Errors associated with the measurements of the slopes and masses of several tenths of a dex in both axes should be considered typical. It should also be noticed that, in many cases, the number of objects in the faintest bins is very small ( $\sim 1 - 2$ ). The effect of unresolved binaries on the MF is estimated by most authors but it does remain as a caveat to keep in mind until much higher spatial resolution observations become available (Kroupa 1995). Mass segregation may also play a role in some cases like the Hyades which may explain the higher than average  $m_c$  for this cluster.

A striking aspect of the results shown in Figure 6 is the similarity between the various MF despite the substantial differences in environment and physical characteristics such as metallicity and age. To be sure there are possible variations and inconsistencies in the details but overall the trend is pretty clear, namely a Salpeter-like increase in numbers with decreasing mass from  $\sim 3 M_\odot$  to  $1 M_\odot$  always followed by a definite break and flattening extending down to  $0.1 - 0.2 M_\odot$  with slopes in the range  $0 < x < 0.5$ . Moreover, all the measurements that reach close to the H-burning limit with reasonable completeness and statistical significance indicate a turnover below  $\sim 0.2 M_\odot$ . Certainly no one simple power-law can possibly explain the data shown in this figure, thus ruling out a scale free IMF in any of these cases.

It is quite conceivable, then, that, at least to the level of accuracy of the present data, all the MF schematically represented in this figure come from basically the same underlying type of distribution function that increases with mass from the substellar limit to a peak somewhere between 0.2 and 0.5 solar masses and then drops steeply beyond  $\sim 1 M_\odot$ . More specifically, convolving a log-normal distribution function with the limited mass resolution and counting statistics presently available could easily generate the segmented power law MF shown in Figure 6. In other words, there seems to be no reason to think that the shape of the IMF from which the various samples are taken is much different from a log-normal implied by the globular cluster data. It is possible that all the MF of the clusters shown in Figure 6 could be the result of a single log-normal since the evident cluster to cluster scatter of peak mass could be completely due to measurement error or systematic effects like mass segregation. In this case, the log-normal implied by the globular cluster data would be a truly universal function essentially independent of age or metallicity.

Another possibility is that this scatter is real and related to some fundamental characteristic of the cluster. The small number of clusters for which reliable MF have been obtained so far precludes, for the moment, precise conclusions such as whether or not there is a trend for  $m_c$  in clusters to increase with age as one might be attempted to deduce from the data in Figure 6. Moreover, there is a group of embedded clusters like  $\rho$  Oph and NGC 2024 that do show a steadily rising MF all the way from  $\sim 1 M_\odot$  to well below the H-burning limit

at  $\sim 0.08 M_{\odot}$  (Williams et al. 1995; Comeron et al. 1996). These MF taken at face value cannot be reconciled with the log-normal form discussed so far unless their  $m_c$  is located deep in the lower reaches of the brown dwarf regime. The Pleiades themselves seem to have a rising MF with decreasing mass below the H-burning limit even if the stellar part is well represented by a log-normal distribution (Bouvier et al. 1998).

These cases would argue for a non universal IMF which could be sensitive to peculiar physical conditions affecting the formation of very low mass stars and brown dwarfs (Evans 1999; Liebert 1999). It is possible to entertain the idea, for example, that physical conditions in dense, massive clusters like the ONC or the globular clusters discussed here are not conducive to their formation. Because there are many open issues surrounding the accurate determination of MF in embedded clusters by means of LF modelling (Luhman et al. 1998; Meyer et al. 1999), and because it is still difficult to pin down the mass peak in young clusters with great enough accuracy, it is probably still too early to tell if this is a serious hypothesis or not but it does raise at least the very exciting possibility of using the bottom of the MS as a sensitive diagnostic of initial conditions in the original star forming regions.

### 6.3. Comparison with Theory

How plausible is a log-normal distribution of the kind advocated here from a purely theoretical perspective? As first pointed out by Larson (1973) and Zinnecker (1984), when the star formation process depends on a large number of independent physical variables, the resulting IMF can be approximately described by a log-normal distribution function of the form discussed in the previous section. As developed in greater detail recently by Adams & Fatuzzo (1996), the observed values of the mass scale  $m_c$  and the standard deviation  $\sigma$  can even be used to set rough limits on the actual physical variables entering into the theory if, as they claim, the mass of a star is self-determined by the action of an outflow. The values of these two parameters obtained for the globular cluster sample discussed in the previous section are quite consistent with our present, admittedly limited, knowledge of the conditions in the star-forming environment. In general, in this particular formulation of the theory, very low mass stars and brown dwarfs are relatively rare since they require natal clouds having unrealistically low effective sound speeds.

On the other hand, it is well known that the IMF cannot be *completely* described by a log-normal form since it is very unlikely that so many variables are involved in the formation process and the greatest deviations will be in tails at the extremes of the function. Thus, it is still quite plausible theoretically to have cases where the lowest mass end of the IMF deviates even significantly from the log-normal form as in the case of the embedded clusters

NGC 2024 and  $\rho$ Oph discussed above. Hierarchical fragmentation may be quite relevant in setting the form of the IMF in the low mass range discussed in this paper (Larson 1995) and this process also would be expected to yield, in principle, a log-normal IMF under the proper circumstances. Recent numerical simulations of the formation of proto-stellar cores from the collapse of dense, unstable gas clumps and subsequent evolution through competitive accretion and interactions such as those expected in a dense cluster, predict a mass spectrum described by a log-normal function quite similar to the ones derived in Figure 6 (Klessen & Burkert 1999) lending even more support to the idea that these represent the original mass function of these clusters.

A completely different purely mathematical approach taken by Elmegreen (1997, 1999a, 1999b) recently arrives at very similar conclusions as to the form of the underlying stellar IMF. In this formalism, proto-stellar gas is randomly sampled from clouds with self-similar hierarchical structure giving rise to an IMF that looks remarkably similar to the one outlined in the previous section. This includes a power law section at intermediate masses and a flattening and turn-over at low masses due to the inability of gas to form stars below the thermal Jeans mass. Of particular interest in our context here is the natural occurrence of IMF fluctuations of several tenths slope due to random variations around a universal IMF quite similar to those observed for the  $\Delta \log N$  of our cluster sample. This theory would then quite naturally explain the scatter observed in this parameter shown in Figure 5. As more data is gathered, if this finding is confirmed it could be used as a strong constraint on theory. On the other hand, such a scatter acts to obscure or even obliterate any sign of possible tidal effects on the MF and again explains why these effects are not at all evident in the data shown in Figure 5. Since the thermal Jeans mass does depend somewhat on environmental conditions, this theory might also be able to explain the possible inter-cluster variation of  $m_c$  seen in Figures 3 and 6.

## 7. Summary and Conclusions

We have analyzed in detail the implications for the IMF of our present reasonably good knowledge of the MS LF of a dozen Galactic globular clusters covering a wide range of physical and orbital characteristics. We have shown, first, that they can be converted to a MF by the application of a ML relation that incorporates all the relevant internal and atmospheric physics of low mass low metallicity stars appropriate to the cluster sample under investigation. We have, then, calculated the possible effect of mass segregation due to energy equipartition on the locally derived MF and find that for nine of the twelve clusters no correction is required as they were obtained very close to the half-light radius where the

deviation is negligible. For the other three clusters, corrections are applied that reduce the observed number gradient between  $0.7 M_{\odot}$  and the mass peak.

The MF obtained in this way could all descend from the same log-normal form of the global MF within a small range of mass scales and standard deviation. The MF of the four clusters of the sample whose LF extend significantly beyond the mass peak at  $0.33 M_{\odot}$  cannot be reproduced by a single power law throughout the MS mass range explored in this paper, but would require at least an unphysical double power law. We, then, explored the possible modification of these global MF with orbital history of the individual clusters by comparing the number gradient of their MF with theoretical estimates of their survivability in the Galactic potential. No statistically significant effect is found, no matter what particular model is used. We conclude that the effect, if present at all in this type of clusters, is completely obscured by the present observational uncertainties and that, therefore, the global MF we measure today must be, within those uncertainties, identical to the original MF namely the IMF.

We explored, finally, the plausibility of this conclusion by examining the measured structure of the MF of much younger clusters that could shed light on the shape of the original globular cluster MF. For many of the best measured clusters, we find convincing evidence that they also exhibit a log-normal shaped IMF in the stellar mass range of the same type deduced from the globulars, albeit, possibly, with a wider range of mass scales and standard deviations. Both the shape and the scatter are roughly consistent with presently available theoretical models. A few deeply embedded clusters do show evidence of possible deviations from this result although there are still some questions as to the validity of the measurement techniques in these difficult environments.

Thus, the conclusion seems robust at this point that most cluster stars originate from a quasi-universal IMF below  $1 M_{\odot}$  having the shape of a log-normal whose precise mass scale and standard deviation may fluctuate from one particular environment to another due to the effects of random sampling or differing physical conditions depending on which model is appropriate. It is also clear that much remains to be done to clarify and establish the range of validity of this conclusion and to understand the origin of the possible deviations such as those found for some embedded clusters. This investigation should yield a bountiful harvest of information on the stellar IMF in the near future. Of particular importance in this endeavour, will be securing a sufficiently large, clean sample of stars of the same physical and kinematical type in a wide variety of environments and ages and to develop the most accurate models of their energy output as a function of mass.

We would like to thank France Allard, Isabelle Baraffe, Santi Cassisi, Gilles Chabrier,

Dana Dinescu, Bruce Elmegreen, Oleg Gnedin, Pavel Kroupa, and Simon Portegies Zwart for useful discussions and an anonymous referee for comments and suggestions that significantly strengthened the paper. We are particularly grateful to Luigi Pulone for having computed the effects of mass segregation on the MF of the clusters in our sample.

## REFERENCES

- Adams, F.C., and Fatuzzo, M. 1996, *ApJ*, 464, 256
- Alexander, D., Brocato, E., Cassisi, S., Castellani, V., Ciaccio, F., and Degl’Innocenti, S. 1997, *A&A*, 317, 90
- Baraffe, I., Chabrier, G., Allard, F., and Hauschildt, P. 1997, *A&A*, 327, 1054
- Baraffe, I., Chabrier, G., Allard, F., and Hauschildt, P. 1998, *A&A*, 337, 403
- Bouvier, J., Stauffer, J.R., Martin, E.L., Barrado y Navascues, D., Wallace, B., and Bejar, V.J.S. 1998, *A&A*, 336, 490
- Capriotti, E.R., and Hawley, S.L. 1996, *ApJ*, 464, 765
- Carretta, E., et al. 1999, in preparation
- Cassisi, S. 1999, private communication
- Chabrier, G., Baraffe, I., Allard, F., and Hauschildt, P. 1999, in *From Extrasolar Planets to Brown Dwarfs*, ESO Conf. Proc., VLT Opening Symposium, ed. F. Paresce, astro-ph/9905210
- Chabrier, G., Baraffe, I., and Plez, B. 1996, *ApJ*, 459, 91
- Chabrier, G., and Méra, D. 1997, *A&A*, 328, 83
- Combes, F, Leon, S., and Meylan, G. 1999, *A&A*, in press
- Comeron, F., Rieke, G.H., and Rieke, M.J. 1996, *ApJ*, 473, 294
- Cool, A. M., Piotto, G., and King, I. R. 1996, *ApJ*, 468, 655
- Dahn, C., Liebert, J., Harris, H.C., and Guetter, H.H. 1995, in *The bottom of the Main Sequence and Beyond*, ESO Conf. Proc., ed. C.G. Tinney (Berlin: Springer), 239
- D’Antona, F., and Mazzitelli, I. 1996, *ApJ*, 456, 329
- Dauphole, B., Geffert, M., Colin, J., Ducourant, C., Odenkirchen, M., and Tucholke, H.J. 1996, *A&A*, 313, 119
- De Marchi, G. 1999, *AJ*, 117, 303
- De Marchi, G., and Paresce, F. 1995a, *A&A*, 304, 202

- De Marchi, G., and Paresce, F. 1995b, *A&A*, 304, 211
- De Marchi, G., and Paresce, F. 1996, in *Science with the Hubble Space Telescope - II*, Eds. P. Benvenuti, F.D. Macchetto, & E. Schreier (Baltimore: STScI), 310
- De Marchi, G., and Paresce, F. 1997, *ApJ*, 476, L19
- De Marchi, G., Paresce, F., and Pulone, L. 2000, *ApJ*, Feb 10 issue, astro-ph/9908251
- De Marchi, G., Leibundgut, B., Paresce, F., and Pulone, L. 1999, *A&A*, 343, L9
- Dinescu, D.I., Girard, T.M., and Van Altena, W.F. 1999, *AJ*, 117, 1792
- Djorgovski, S. 1993, in *Structure and Dynamics of Globular Clusters*, ASP Conf. Ser. 50, ed. S. Djorgovski and G. Meylan (San Francisco: ASP), 373
- Drukier, G.A., Slavin, S.D., Cohn, H.N., Lugger, P.M., Barrington, R.C., Murphy, B.W., and Seitzer, P.O 1998, *AJ*, 115, 708
- Elmegreen, B.G. 1997, *ApJ*, 486, 944
- Elmegreen, B.G. 1999a, in *Unsolved Problems in Stellar Evolution*, ed. M. Livio (Cambridge: Cambridge University Press), in press, astro-ph/9811289
- Elmegreen, B.G. 1999b, *ApJ*, 515, 323
- Elson, R.A.W., Gilmore, G.F., Santiago, B.X., Casertano, S. 1995, *AJ*, 110, 682
- Evans, N.J. 1999, astro-ph/9905050
- Ferraro, F.R., Carretta, E., Bragaglia, A., Renzini, A., and Ortolani, S. 1997, *MNRAS*, 286, 1012
- Fuchs, B., and Jahreiss, H. 1998, *A&A*, 329, 81
- Gizis, J.E., and Reid, I.N. 1999, *AJ*, 117, 508
- Gizis, J.E., and Reid, I.N., and Monet, D.G. 1999, *AJ*, 118, 997
- Gnedin, O.Y., Hernquist, L., and Ostriker, J. P. 1999, *ApJ*, 514, 109
- Gnedin, O.Y., and Ostriker, J.P. 1997, *ApJ*, 474, 233
- Graff, D., and Freese, K. 1996, *ApJ*, 456, L49
- Gratton, R., Fusi Pecci, F., Carretta, E., Clementini, G., Corsi, C., and Lattanzi, M. 1997, *ApJ*, 491, 749
- Hillenbrand, L.A. 1997, *AJ*, 113, 1733
- Herbig, G. 1998, *ApJ*, 497, 736
- King, I. R., Anderson, J. , Cool, A. M., and Piotto, G. 1998, *ApJ*, 492, L37
- Klessen, R.S., and Burkert, A. 1999, *ApJ*, in press, astro-ph/9904090

- Kroupa, P. 1995, MNRAS, 277, 1522
- Larson, R.B. 1973, MNRAS, 161, 133
- Larson, R.B. 1995, MNRAS, 272, 213
- Leon, S., Combes, F, and Meylan, G. 1999, A&A, in press
- Liebert, J., 1999, in *Unsolved Problems in Stellar Evolution*, ed. M. Livio (Cambridge: Cambridge University Press), in press, astro-ph/9812061
- Luhman, K., Rieke, G.H., Lada, C.J., and Lada, E.A. 1998, ApJ, 508, 347
- Marconi, G., Buonanno, R., Carretta, E., Ferraro, F.R., Fusi Pecci, F., Montergriffo, P., De Marchi, G., Paresce, F., and Laget, M. 1997, MNRAS, 293, 479
- Meyer, M.R., Adams, F., Hillenbrand, L., Carpenter, J., and Larson, R. 1999, in *Protostars & Planet IV*, eds. V. Mannings, A. Boss, and S. Russell (Tucson: The University of Arizona Press), in press
- Meylan, G. 1987, A&A, 184, 144
- Meylan, G. 1988, A&A, 203, 297
- Murali, C., and Weinberg, M.D. 1997, MNRAS, 291, 717
- Odenkirchen, M., Brosche, P., Geffert, Tucholke, H.J. 1997, NewA, 2, 477
- Paresce, F., De Marchi, G., and Romaniello, M. 1995, ApJ, 440, 216
- Piotto, G. , Cool, A. M., and King, I. R. 1997, AJ, 113, 1345
- Piotto, G., and Zoccali, M., 1999, A&A, 345, 485
- Pont, F., Mayor, M., Turon, C., and Vandenberg, D.A. 1998, A&A, 329, 87
- Pryor, C., Smith, G.H., and McClure, R.D. 1986, AJ, 92. 1358
- Pulone, L., De Marchi, G., and Paresce, F. 1999, A&A, 342, 440
- Richer, H.B., Fahlman, G., Buonanno, R., Fusi Pecci, F., Searle, L., and Thompson, I. 1991, ApJ, 381, 147
- Rood, R.T., Carretta, E., Paltrinieri, B., Ferraro, F.R. Fusi Pecci, F., Dorman, B., Chieffi, A., Straniero, O., Buonanno, R. 1999, ApJ, 523, 752
- Rubenstein, E.P., and Bailyn, C.D, 1999, ApJ, 513, L33
- Scalo, J.M. 1998, in *The Stellar Initial Mass Function*, ASP Conf. Ser. 142, eds. G. Gilmore and D. Howell (San Francisco: ASP), 201
- Scalo, J.M. 1999, in *The Birth of Galaxies*, Blois, France, astro-ph/9811341
- Silvestri, F., Ventura, P., D'Antona, F., and Mazzitelli, I. 1998, ApJ, 509,192

- Takahashi, K., and Portegies Zwart, S. 1999, ApJ, submitted, astro-ph/9903366
- Vesperini, E. 1998, MNRAS, 299, 1019
- Vesperini, E. 1997, MNRAS, 287, 915
- Vesperini, E., and Heggie, D.C. 1997, MNRAS, 289, 898
- Webbink, R.F. 1985, IAU Symp, 113, 541
- Williams, D.M., Comeron, F., Rieke, G.H., and Rieke, M.J. 1995, ApJ, 454, 144
- Zinnecker, H. 1984, MNRAS, 210, 43

Table 1: The clusters in our sample. Columns 3 and 4 show the radial distance at which the LF have been measured, respectively in arcmin and in units of the half-light radius ( $r_h$ ; see Table 2). LF have been measured within  $\pm 1 r_h$  of the given average position  $r$ .

NGC	Name	$r$	$r/r_h$	Reference
104	47 Tuc	4.6	1.6	De Marchi & Paresce (1995b)
5139	$\omega$ Cen	4.6	0.9	De Marchi (1999)
5272	M 3	1.5	1.5	Marconi et al. (1997), Carretta et al. (1999)
6121	M 4	6.1	1.3	Pulone, De Marchi & Paresce (1999)
6254	M 10	2.4	1.3	De Marchi & Paresce (1996)
6341	M 92	4.6	4.5	Piotto, Cool & King (1997)
6397		4.6	1.8	Paresce, De Marchi & Romaniello (1995)
6656	M 22	2.6	0.8	De Marchi & Paresce (1997)
6752		3.1	1.5	Ferraro et al. (1997)
6809	M 55	2.5	0.9	De Marchi & Paresce (1996)
7078	M 15	4.6	4.6	De Marchi & Paresce (1995a)
7099	M 30	4.6	4.6	Piotto, Cool & King (1997)

Table 2. Clusters’ structural parameters

NGC	$(m-M)_I$	$r_h$	$r_c$	$c$	$Z_G$	$R_G$	$P$	[Fe/H]	$T_d$	$T_d$	$m_c$	$\sigma$	$\Delta \log N$
(1)	(2)	(3)	(4)	(5)	(6)	(7)	(8)	(9)	(10)	(11)	(12)	(13)	(14)
104	13.37	2.9	0.2	2.48	3.2	7.4	5.3	-0.71	88	131	0.34	2.11	0.131
5139	13.68	4.9	2.6	1.15	1.3	6.3	1.2	-1.59	40	16	0.37	1.96	0.122
5272	15.03	1.2	0.4	1.89	10.0	12.0	5.5	-1.66	213	275	0.36	1.61	0.251
6121	12.11	4.5	1.2	1.53	0.5	6.2	0.7	-1.33	13	2	0.32	1.84	0.208
6254	13.59	1.9	0.7	1.66	1.7	4.7	3.4	-1.60	22	23	0.33	2.19	0.136
6341	14.41	1.0	0.3	1.65	4.3	9.1	1.4	-2.24	30	33	0.30	1.73	0.104
6397	12.00	2.9	0.1	1.69	0.5	6.0	3.1	-1.91	4	4	0.32	1.73	0.237
6656	12.93	3.3	1.2	1.70	0.4	5.1	2.9	-1.75	31	29	0.33	1.73	0.218
6752	13.18	2.0	0.5	2.15	1.8	5.1	4.8	-1.54	35	96	0.42	1.84	0.089
6809	13.57	2.7	1.7	1.27	1.9	4.2	1.8	-1.82	14	11	0.32	1.68	0.250
7078	15.19	1.0	0.1	1.77	4.8	10.5	5.5	-2.17	48	155	0.30	1.50	0.140
7099	14.43	1.0	0.1	2.40	5.4	6.8	3.2	-2.13	23	40	0.30	1.84	0.159

Note. — Columns are as follows: (1) NGC number; (2) distance modulus in the  $I$  band defined as  $(m - M)_V + 0.48A_V$ , with the latter two values taken from Djorgovski (1993); (3) half-light radius in arcmin (Djorgovski 1993); (4) and (5) core radius in arcmin and concentration ratio (Webbink 1985); (6) and (7) distance in kpc respectively from the Galactic plane and center (Djorgovski 1993); (8) perigalactic distance in kpc (Dinescu et al. 1999); (9) metallicity (Djorgovski 1993); (10) and (11) time to disruption in Gyr (assuming  $T_0 = 10$  Gyr) respectively from Gnedin & Ostriker (1997) and Dinescu et al. (1999); (12) and (13) average characteristic mass (solar units) and standard deviation of the log-normal distribution that best fits the MF; (14) logarithmic ratio  $\Delta \log N$  of lower to higher mass stars as defined in Section 3.

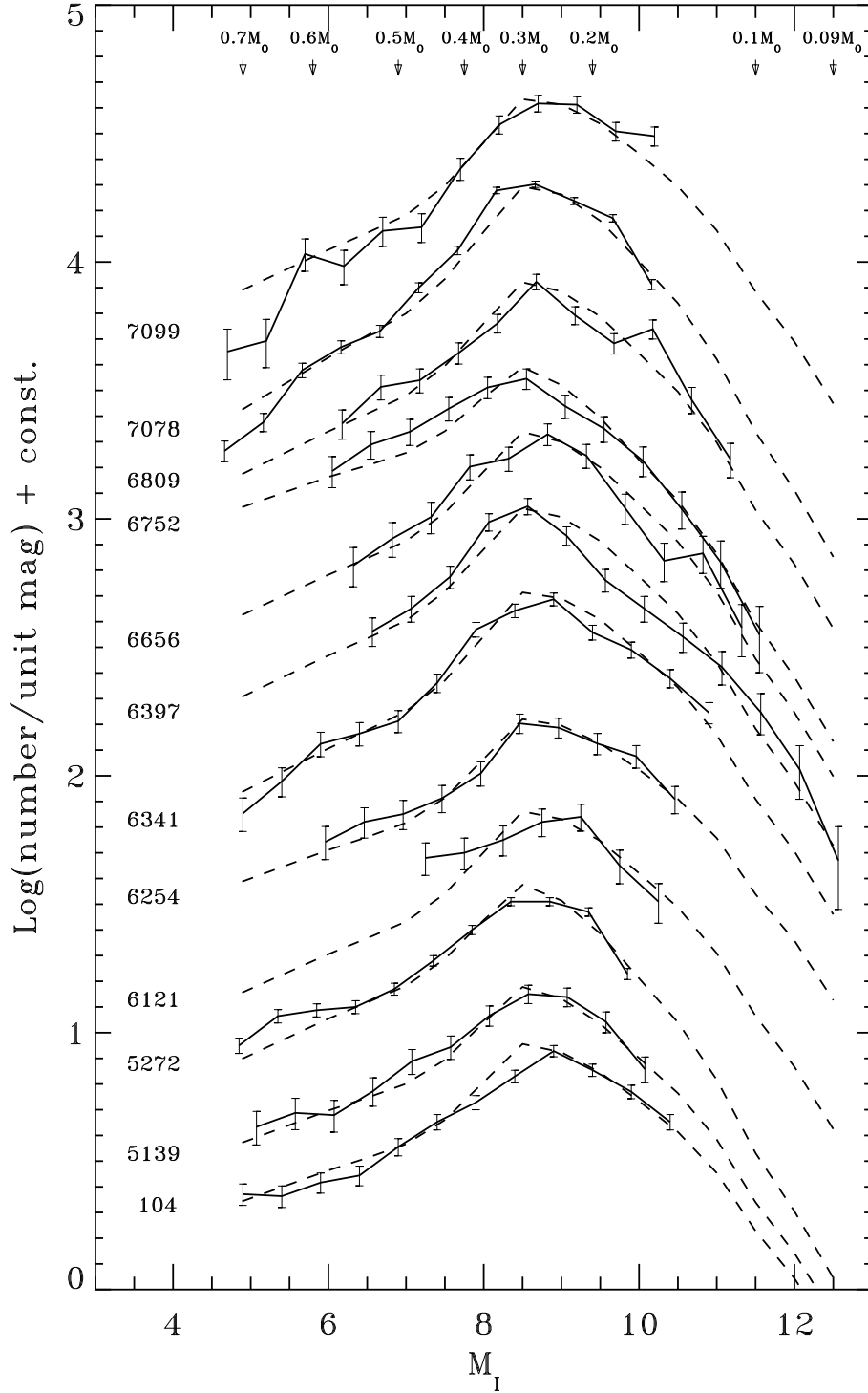


Fig. 1.— Luminosity functions of the clusters in our sample (see Table 1). The data have been shifted vertically by an arbitrary amount for enhanced visibility. The mass values shown at the top are taken from Baraffe et al. (1997) for  $[M/H] = -1.5$ . The dashed lines show the result of folding the log-normal MF of Figure 3 through the ML relation of Baraffe et al. (1997; see Section 3)

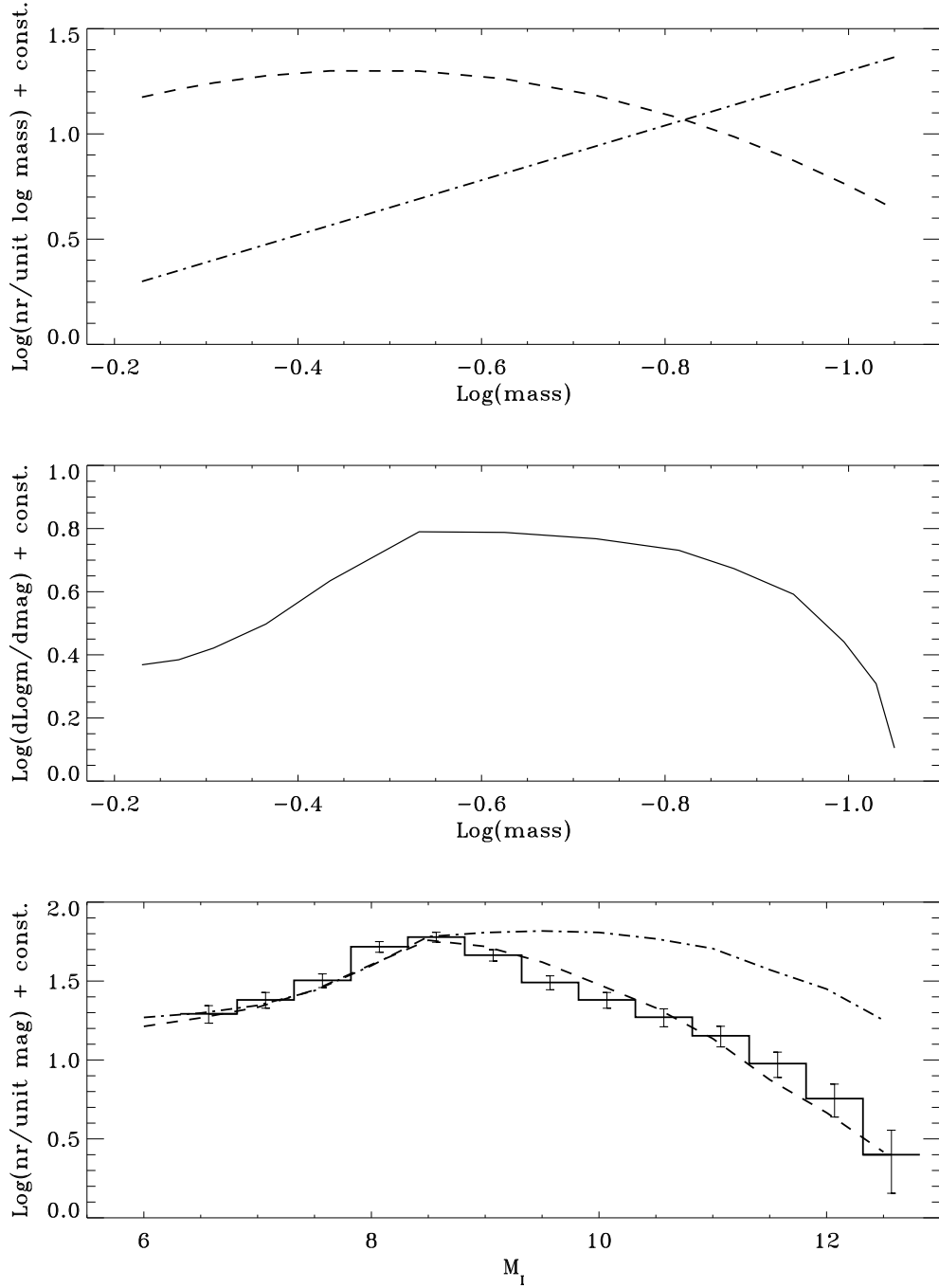


Fig. 2.— Conversion of a mass function into a luminosity function through the mass-luminosity relation. *Top panel:* two MF are used, namely a power-law distribution (dot-dashed line,  $x = 1.3$ ) and a log-normal distribution with  $m_c = 0.32$  and  $\sigma = 1.73$  (dashed line). *Middle panel:* derivative of the M-L relation of Baraffe et al. (1997) for  $[M/H] = -1.5$ . *Bottom panel:* Once multiplied by the derivative of the M-L relation only the log-normal MF (dashed line) fits both the rising and falling portions of the luminosity function simultaneously, whereas the power-law form (dot-dashed line) can only fit one of them, depending on the choice of the exponent.

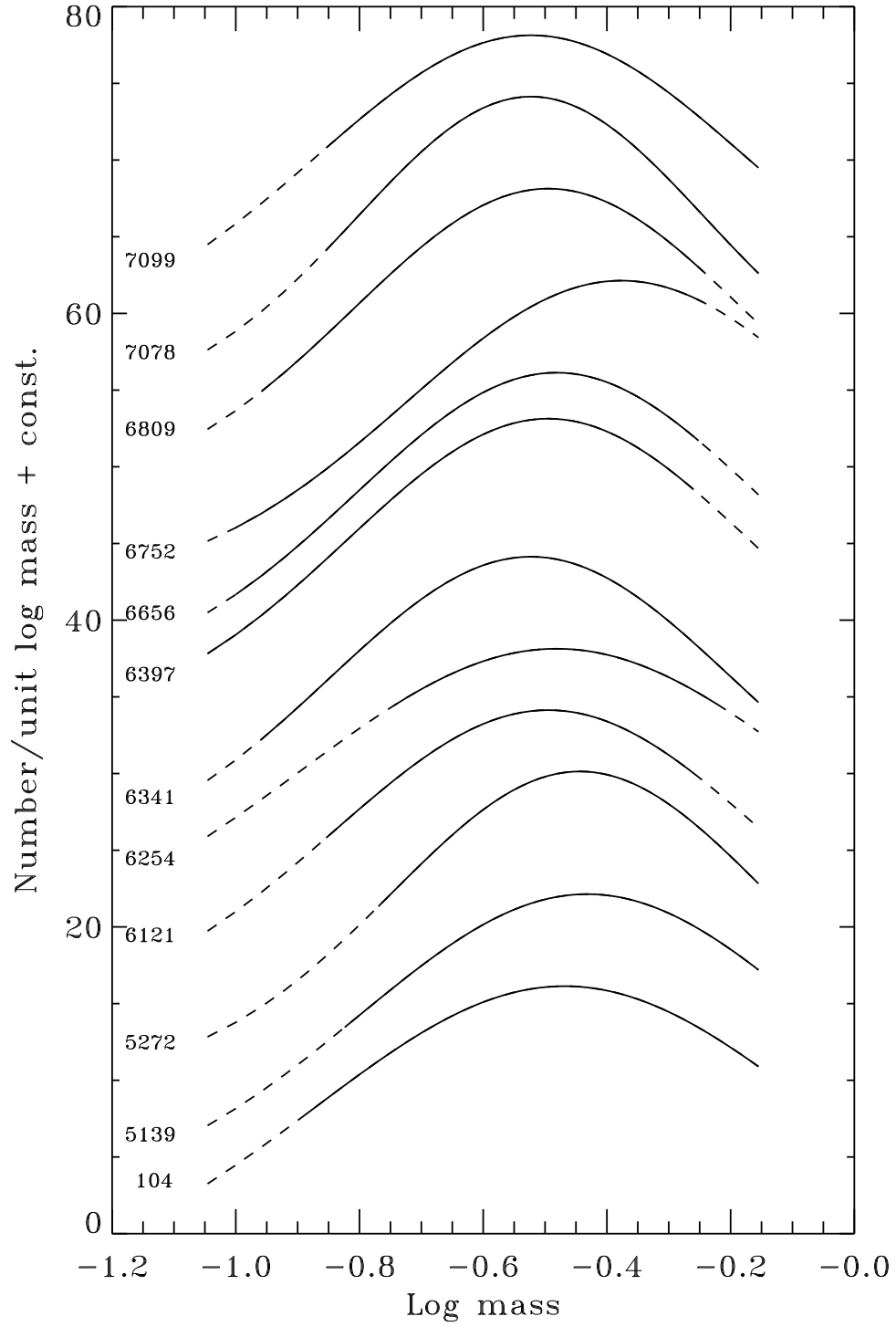


Fig. 3.— Log-normal mass functions that best fit the LF shown in Figure 1. Note that the scale is linear along the y axis.

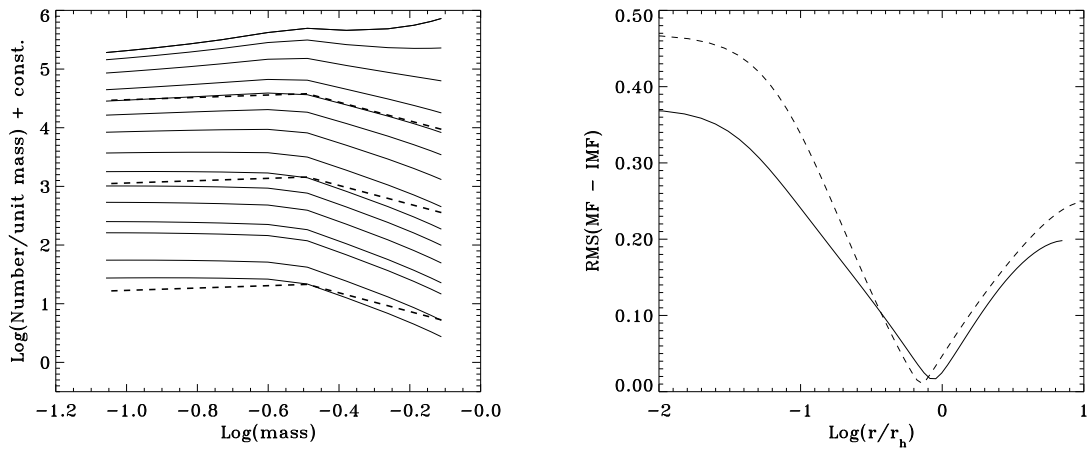


Fig. 4.— Effects of mass segregation on the shape of the MF as predicted by Michie–King models. *Left panel:* The expected local MF is plotted as a function of radial position and compared to the input global MF (dashed lines) for NGC 6397. Radial distances are, from top to bottom, 0, 0.1, 0.3, 0.6, 1, 1.5, 2, 3, 4, 5, 6, 7, 8, 9, 10 times  $r_h$ . *Right panel:* standard deviation of the local from the global MF as a function of radial position for NGC 6397 (solid line) and NGC 104 (dashed line).

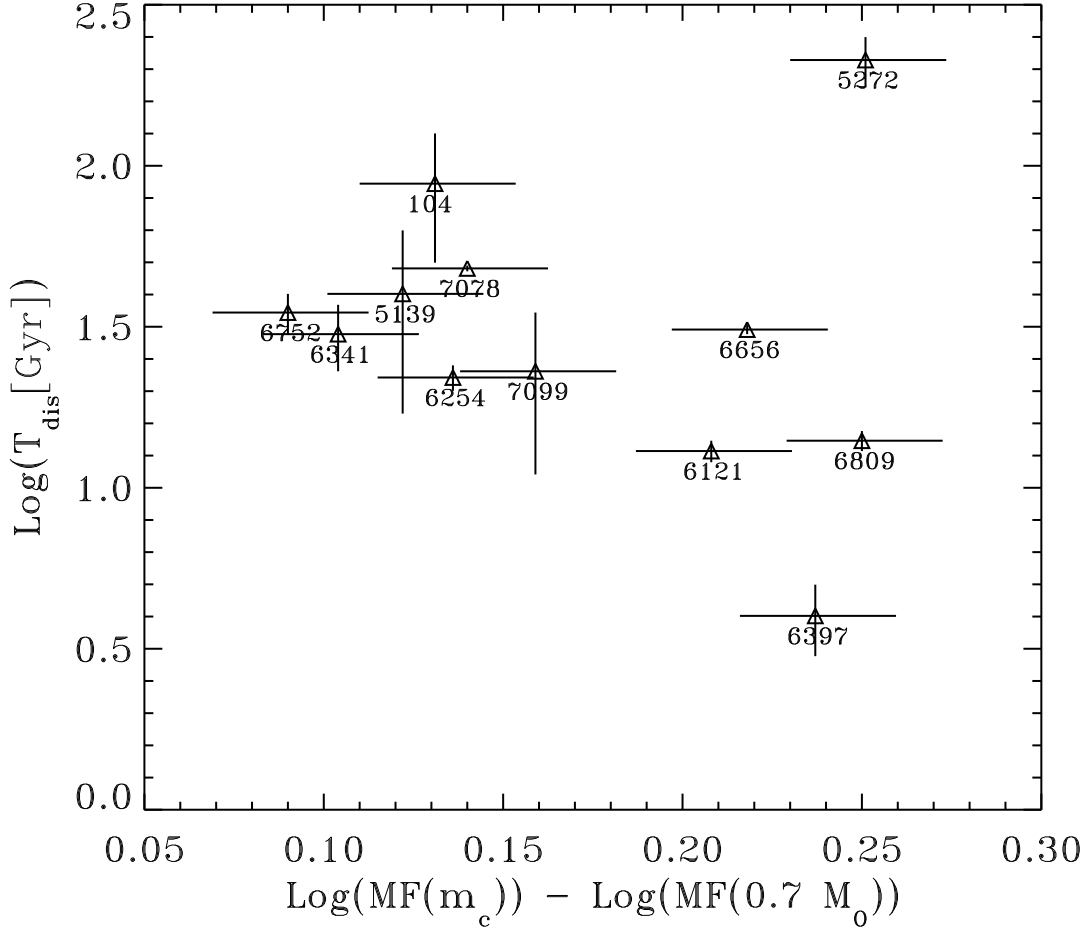


Fig. 5.— The time to disruption in Gyr as calculated by Gnedin & Ostriker (1997) is shown here as a function of the index  $\Delta \log N$  describing the shape of the MF in Figure 3 (see text). Vertical error bars reflect the difference between the values of  $T_d$  obtained with two different models describing the distribution of stars in the Galaxy. Horizontal error bars mark the range in which  $\Delta \log N$  can vary as a result of the uncertainty affecting the values of  $m_c$  and  $\sigma$  in the MF. As such, both error bars define in practice a  $\pm 3 \sigma$  uncertainty.

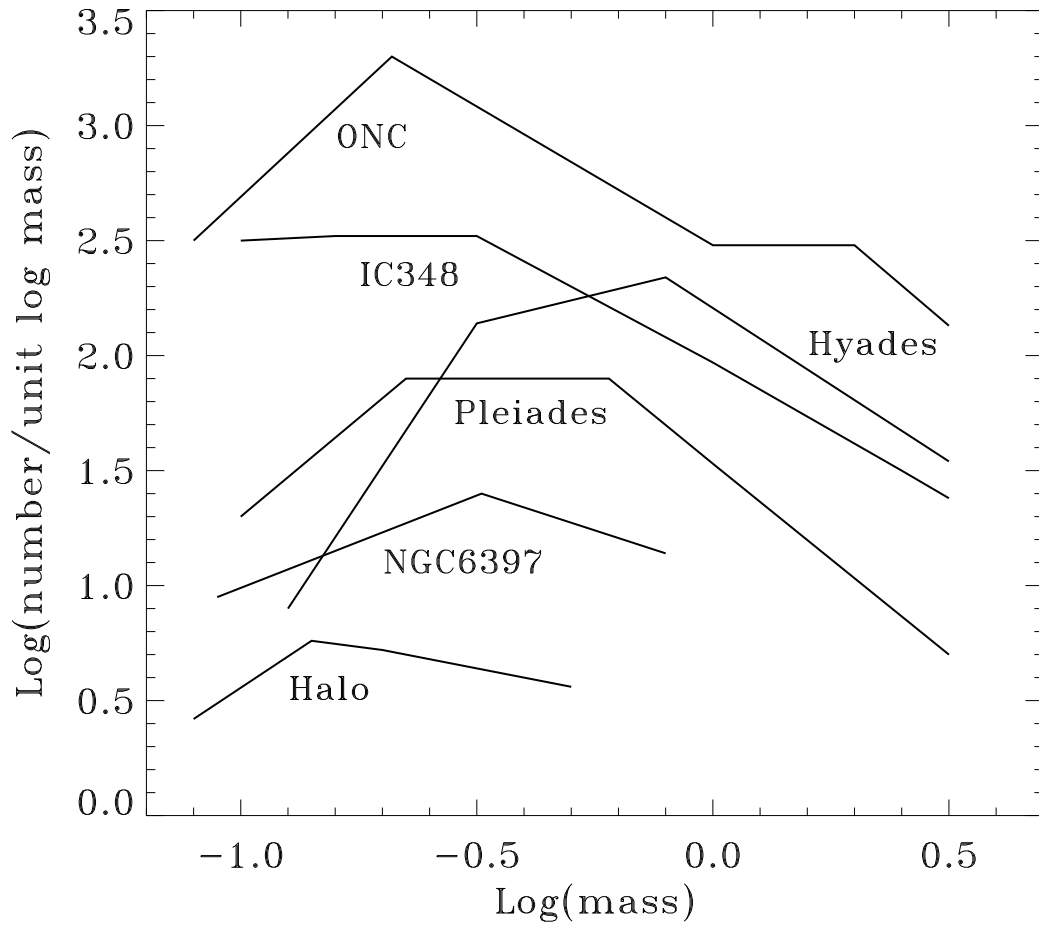


Fig. 6.— Mass function of stars in young open clusters, in the Halo, and in NGC 6397 (see text).